Effect of Micelle Diameter on Tryptophan Dynamics in an Amphipathic Helical Peptide in Phosphatidylcholine

Larry R. McLean,*,‡ John L. Krstenansky,‡ Thomas J. Owen,‡ Maurice R. Eftink,§ and Karen A. Hagaman‡

Merrell Dow Research Institute, 2110 East Galbraith Road, Cincinnati, Ohio 45215, and Department of Chemistry, The University of Mississippi, University, Mississippi 38677

Received April 6, 1989; Revised Manuscript Received June 26, 1989

ABSTRACT: The effect of dimyristoylphosphatidylcholine (DMPC) on the conformation and environment of the single tryptophan residue of a model amphipathic helical polypeptide has been investigated by fluorescence quenching with a water-soluble, neutral quencher (acrylamide) and multiple-frequency phase fluorometry. The peptide H-Ser-Ser-Ala-Asp-Trp-Leu-Lys-Ala-Phe-Tyr-Asp-Lys-Val-Ala-Glu-Lys-Leu-Lys-Glu-Ala-Phe-Ser-Ser-Ser-OH [18As; Kanellis, P., Romans, A. Y., Johnson, B. J., Kercret, H., Chiovetti, R., Jr., Allen, T. M., & Segrest, S. P. (1980) *J. Biol. Chem. 255*, 11464] was synthesized by solid-phase techniques. Peptide was incubated at 26 °C with DMPC at various peptide:lipid weight ratios. The diameter of the resulting disk-shaped micelles increases with increasing lipid concentration from 12.0 ± 0.4 nm at a 1:1 weight ratio of peptide to lipid to a maximum of 48.7 ± 1.0 nm at a 1:13 ratio. At a weight ratio of 1:5, the average diameter is 22.7 ± 0.6 nm. Decreasing the peptide:lipid ratio of the micelle resulted in a blue-shift in the fluorescence emission maximum (from 337 nm at 1:1 to 334 nm at 1:5), an increase in the fluorescence lifetime of the tryptophan measured by the phase shift method at 18 MHz (from 3.12 ns at 1:1 to 3.61 ns at 1:5), a decrease in the rate of fluorescence quenching by acrylamide (from 0.87×10^9 M^{-1} s^{-1} at 1:1 to 0.42×10^9 M^{-1} s^{-1} at 1:5), and an increase in the activation energy for quenching (from 6.7 kcal/mol at 1:1 to 12.7 kcal/mol at 1:5). Multiple-frequency phase fluorometry data obtained on micelles at various peptide:lipid ratios were best fit either by two-exponential lifetime components or by a single Lorentzian distribution of lifetimes. With increasing micelle diameter and decreasing peptide:lipid ratio, the fraction of the longer lifetime component (in a two-component analysis) or the width of the lifetime distribution (in a Lorentzian analysis) is increased. However, the values of the short- (~1 ns) and long- (~4 ns) lifetime components obtained in a two-component analysis of the multifrequency data are relatively independent of peptide:lipid ratio. A global analysis of the data gives $\tau_1 = 4.5$ ns and $\tau_2 = 1.1$ ns; the fraction (f_1) of the longer lifetime component increases monotonically with decreasing peptide:lipid ratio. Lifetime-resolved emission anisotropy measurements were employed to determine the nanosecond rotational motions of the tryptophan residue in the micelles. Decreasing the peptide:lipid ratio from 1:1 to 1:5 had only a minimal effect on the rate of the rapid motions but significantly decreased the fraction of anisotropy which was lost due to faster motions. At a lower peptide:lipid ratio (1:8), the rate of rapid motions was also slowed. Thus, the tryptophan residue in this amphipathic helical peptide in phosphatidylcholine becomes less accessible to the aqueous phase solvent with decreasing peptide:lipid ratio, which corresponds to increasing micelle diameter.

The amphipathic helix, a common structural feature of many proteins which bind to phospholipids, is defined as an α-helical region of a protein in which the amino acid residues are distributed in the secondary structure to form opposing polar and nonpolar faces. The amphipathic helix was first recognized in myoglobin by Perutz et al. (1965). In 1969, Day and Levy proposed that an amphipathic helical structure, in which the polar residues on one side of the helix interact with the polar portion of the phospholipids and the nonpolar residues on the opposite side interact with the acyl chains of the lipid, might account for lipid–protein interactions in the apolipoproteins of plasma lipoproteins. When the first sequences of the apolipoproteins were obtained, Segrest et al. (1974) found that amphipathic helical surfaces could be formed in several regions of each of the apolipoproteins. Recently, the amphipathic helix has been proposed as an important structural feature of several peptide hormones (Kaiser & Kezdy, 1984) and cytotoxic peptides (Argiolas & Pisano, 1985).

Considerable data are available on the effects of lipid binding on the structure of amphipathic helical proteins [see Morrisett et al. (1977) for a review of the early literature]. Addition of lipid to the soluble plasma apolipoproteins, or to amphipathic peptides, generally results in an increase in the α-helicity and a blue-shift in the fluorescence emission maximum of the peptide. Fluorescence quenching experiments have shown a decrease in solvent exposure of the tryptophan residue in several of the apolipoproteins upon binding to lipid (Morrisett et al., 1977; Maliwal et al., 1985; Mantulin et al., 1986). However, less attention has been paid to the mechanism of fluorescence quenching or to the details of the tryptophan environment of amphipathic helical peptides within lipid micelles. Since all collisions of acrylamide with tryptophan residues in the excited state result in quenching, buried tryptophan residues in proteins are quenched as a result of fluctuations in the structure of the protein (Eftink & Ghiron, 1976). Whether such a mechanism applies to peptide–lipid micelles is not clear.

The present report is directed toward a description of the tryptophan environment of a model amphipathic peptide

‡ Merrell Dow Research Institute.
§ The University of Mississippi.

0006-2960/89/0428-8403$01.50/0 © 1989 American Chemical Society

(18As; Kanellis et al., 1980) in phosphatidylcholine micelles. This peptide forms disk-shaped micelles with a diameter that depends upon the ratio of protein to lipid (Anantharamaiah et al., 1985) as do many of the apolipoproteins (Tall et al., 1977; Swaney, 1980; Jonas et al., 1980; Massey et al., 1981; Brouillette et al., 1984). A progressive downfield shift of the choline *N*-methyl proton resonance of the lipid head groups and a decrease in the enthalpy of the lipid-phase transition in micelles of 18As in phosphatidylcholine have been observed with increasing micelle diameter (Anantharamaiah et al., 1985). Although multiple-lifetime components and nanosecond motions of peptides and proteins in lipid have been reported (Masotti et al., 1986; Jonas et al., 1982; Maliwal et al., 1985; Georghiou et al., 1982), the effect of micelle size or lipid:peptide ratio on the conformation of peptides or proteins in lipid micelles is not well understood. For apoA-I/1,2-dimyristoylphosphatidylcholine (DMPC),[1] micelles, the diameter of the micelles had no effect on the CD and fluorescence spectra of the apoprotein (Jonas et al., 1980). Since apoA-I is a multi-tryptophan protein, interpretation of structural data in terms of a general model for the interactions of amphipathic helical peptides with lipid is limited. In the present report, acrylamide quenching, multiple-frequency phase fluorometry, and lifetime-resolved emission anisotropy data have been used to elicit information on the solvent accessibility and dynamics of the single tryptophan residue of a model amphipathic helical peptide in DMPC as a function of peptide:lipid ratio. The data show that the rate and activation energy of fluorescence quenching by acrylamide, the distribution of fluorescence lifetimes, and the rotational dynamics of the tryptophan residue systematically vary with the peptide:lipid ratio of the micelle.

Experimental Procedures

Materials. 1,2-Dimyristoyl-*sn*-glycero-3-phosphocholine (DMPC) (Avanti Polar Lipids), N^{α}-acetyl-L-tryptophanamide, *p*-terphenyl (Aldrich, Gold Label), and acrylamide (Bio-Rad, ultrapure) were used without further purification. Standard buffer was 10 mM Tris-HCl/1 mM ethylenediaminetetraacetic acid, pH 7.40. 1,2-Di[1-^{14}C]myristoylphosphatidylcholine (108 mCi/mmol) was obtained from Amersham.

Synthesis and Purification of Peptide. The 24-residue peptide H-Ser-Ser-Ala-Asp-Trp-Leu-Lys-Ala-Phe-Tyr-Asp-Lys-Val-Ala-Glu-Lys-Leu-Lys-Glu-Ala-Phe-Ser-Ser-Ser-OH [18As (Kanellis et al., 1980)] was synthesized by solid-phase techniques on Boc(Bzl)SerPAM resin (0.75 mmol/g) using an applied Biosystems Model 430A peptide synthesizer. All residues were double-coupled as their N^{α}-*t*-Boc-blocked symmetrical anhydrides. The side-chain protection was as follows: Asp(Chx), Glu(Chx), Lys(2-ClZ), Ser(Bzl), Trp(For), Tyr(2-BrZ). The peptide was deprotected and cleaved from the resin by treatment with HF/anisole/ethanedithiol (85:10:5) at 0 °C for 45 min. After removal of the HF in vacuo, the peptide was precipitated with ether and extracted with 30% aqueous acetic acid. The extract was lyophilized, and the residue was eluted on a column (2.6 × 92 cm) of Sephadex G-15 (30 mL/h) monitored at 254 nm. The major peak was collected, lyophilized, and purified by reverse-phase high-performance liquid chromatography (HPLC) with a Vydac 218TP1010 C18 column (10 × 250 mm) at 35% CH_3CN in 0.1 aqueous trifluoroacetic acid. The major peak was collected and lyophilized. Identity and purity were confirmed by amino acid analysis, mass spectrometry (FAB-MS), HPLC, and thin-layer chromatography (TLC). Amino acid analyses (HCl digest, 106 °C, 20 h, uncorrected for decomposition) gave Asx 1.72 (2), Ser 4.09 (5), Glx 1.92 (2), Ala 4.29 (4), Val 1.00 (1), Leu 2.08 (2), Tyr 0.93 (1), Phe 2.06 (2), and Lys 4.05 (4); enzyme digest, leucine aminopeptidase (Sigma), 40 °C, 24 h gave Asp 1.99 (2), Ser 4.94 (5), Glu 2.07 (2), Ala 3.90 (4), Val 1.03 (1), Leu 2.03 (2), Tyr 1.04 (1), Phe 2.04 (2), and Lys 3.98 (4). FAB-MS gave the molecular ion $(M + H)^+ = 2707$ (calcd M_r 2706.4) with some fragmentation confirming the sequence. In isocratic 35% acetonitrile in 0.1% trifluoroacetic acid, $k' = 3.40$. Peptide was analyzed by TLC (0.05 and 0.1 mg of sample) on silica gel 60 F_{254} (Merck, 0.25 mm, 20 × 20 cm) and was visualized by iodine, ninhydrin, and chlorine tolidine. In the solvent system 1-butanol/acetic acid/water/pyridine (60:12:48:60), R_f = 0.41, in 2-propanol/ammonium hydroxide/water (3:1:1), R_f = 0.24, and in 1-butanol/acetic acid/water (4:5:5), R_f = 0.59. The final product was >97% pure by analytical HPLC. HPLC on a Vydac 218TP54 (4.6 × 250 mm) C18 column, with a 25–50% linear gradient of acetonitrile in 0.1% trifluoroacetic acid over 25 min at 2.0 mL/min, t_0 = 1.95 min, gave a single peak with a retention time of 17.05 min.

Preparation of Peptide–Lipid Micelles. DMPC (1 mg) was dissolved in chloroform and dried under N_2 on the walls of a test tube, lyophilized for 30–60 min, and incubated in 1 mL of standard buffer for 1 h at 30 °C. After being vortexed, dry peptide was added to the liposomes to give various weight ratios of peptide to DMPC. The mixtures were vortexed and incubated at 24 °C for 24–48 h under N_2. The formation of micelles was monitored by the absorbance at 400 nm after addition of peptide. At peptide:lipid weight ratios of 1:1 and 1:2, the optical density of the mixtures was constant after 30 min. At higher lipid concentrations, the absorbance of the initially turbid liposomes decreases more slowly, requiring 6 h at a peptide:lipid ratio of 1:13. All mixtures were visually clear at ratios from 1:2 to 1:13 after 6 h of incubation at 24 °C. The resulting clear mixtures were dialyzed against standard buffer at 24 °C. All fluorescence measurements were made at a constant concentration of 0.1 mg of peptide/mL.

Electron Microscopy. Samples were diluted in 10 mM Tris-HCl, pH 7.4, and placed on grids with nitrocellulose/carbon or Formvar films. The samples were negatively stained with 2% (w/v) sodium phosphotungstic acid, pH 7.4, and examined on a JOEL-100CX-II electron microscope at 20000–100000× magnification. The width of 30 stacks of micelles at each peptide:lipid ratio was measured from electron micrographs with the aid of an ocular magnifier with metric rule.

Fluorescence Measurements. DPH polarization was measured as described previously (McLean & Hagaman, 1988). Fluorescence lifetimes were measured by the phase-modulation technique (Spencer & Weber, 1969). A modulation frequency of 18 MHz was achieved with a Debye–Sears modulator on an SLM 4800 spectrofluorometer. Lifetime measurements at modulation frequencies from 10 to 180 MHz were made with an SLM 4800 equipped with a Pockel cell modulator (Industria Strumentazioni Scientifiche, Champaign, IL). The exciting light passed through either an excitation monochromator (bandwidth 0.5 nm) or an excitation filter centered at 289 nm (bandwidth 10 nm, Melles Griot F1M022). Emission was observed either through an Ealing 35-2997 interference filter (center 340 nm, bandwidth 12 nm) or through a Corning 7-60 filter. The standard deviations of the phase and modulation measurements were 0.6 and 0.01, respectively. A so-

[1] Abbreviations: DMPC, 1,2-dimyristoylphosphatidylcholine; CD, circular dichroism.

lution of *p*-terphenyl in absolute ethanol was used as reference. Solutions were equilibrated for 30 min at the temperature of measurement. Fluorescence intensities remained constant for at least 60 min at all temperatures studied. Measurements of lifetimes with a vertically oriented excitation polarizer and an emission polarizer at 55° were within the standard deviation of the phase lifetime measurements without polarizers, indicating minimal influence of light scattering on the lifetime values.

Fluorescence Quenching. In quenching experiments, fluorescence intensities and phase lifetimes (18 MHz) were measured with excitation at 295 nm (0.5-nm bandwidth); emission was observed through an Ealing 35-2997 interference filter. Acrylamide quenching was observed after adding aliquots of an 8 M acrylamide solution to peptide or micelles in the same buffer. Corrections for absorptive screening were made as described by Parker (1968) with $\epsilon = 0.25\ M^{-1}$ for acrylamide. The standard deviation of the lifetime measurements was <0.03 ns.

Quenching data were analyzed according to the modified Stern–Volmer equation (Eftink & Ghiron, 1976):

$$F_0/[F \exp(V[Q])] = 1 + K_{sv}[Q] \quad (1)$$

where F_0 and F are the fluorescence intensities in the absence and presence of quencher, [Q] is the molar concentration of quencher, V is the static (exponential) quenching constant, and K_{sv} is the dynamic (Stern–Volmer) quenching constant. K_{sv} is equal to $k_q\tau_0$ where k_q is the rate constant for the quenching reaction (and is an index of exposure of fluorophores in proteins) and τ_0 and τ are the fluorescence lifetimes of the fluorophore in the absence and presence of quencher, respectively. V is related to the probability of finding a quencher molecule in the immediate vicinity of the fluorophore at any time. Fluorescence intensity data were analyzed by fitting F vs [Q] data by a nonlinear least-squares procedure to obtain K_{sv} and V from $F = F_0/\{(1 + K_{sv}[Q]) \exp(V[Q])\}$. Lifetime data were analyzed similarly with $\tau = \tau_0/(1 + K_{sv}[Q])$. Initial parameters for the nonlinear fit were estimated from the slope of F_0/F or τ_0/τ vs [Q], with $V = 0$. The collisional quenching constant, k_q, was calculated from K_{sv} and the fluorescence phase lifetime at 18 MHz. Activation energies were calculated from the expression $k_q/T = A \exp(-E_a/RT)$, where T is temperature, A is a preexponential constant, and R is the molar gas constant, by fitting a line to an Eyring plot of ln (k_q/T) vs $1/T$ by linear regression.

Fluorescence Lifetimes. The impulse–response function of the fluorescence samples for a discrete distribution is given by (Lakowicz et al., 1984; Jameson et al., 1984)

$$F(t) = \sum \alpha_i \exp(-t/\tau_i) \quad (2)$$

where τ_i is the fluorescence lifetime, t is time, and α_i is the preexponential constant. The sum is over one component for a single-exponential decay or two components for a double-exponential decay. The fractional intensity is given by $f_i = \alpha_i\tau_i/\sum\alpha_i\tau_i$. The average lifetime $\langle\tau\rangle = \sum f_i\tau_i$. For a continuous distribution of lifetimes:

$$F(t) = \int_0^\infty f(\tau)\tau^{-1} \exp(-t/\tau)/\tau \, d\tau \quad (3)$$

where $f(\tau)$ is a probability density function. A Lorentzian probability density distribution was used to model the present data set (Alcala et al., 1987). The frequency (ω)-dependent phase angle and modulation are given by

$$\phi(\omega) = \tan^{-1}[S(\omega)/G(\omega)] \quad (4)$$

$$M(\omega) = [1 + S(\omega)^2G(\omega)^2]^{-1/2} \quad (5)$$

where

$$S(\omega) = \int_0^\infty F(t) \sin(\omega t)\, dt / \int_0^\infty F(t)\, dt \quad (6)$$

$$G(\omega) = F(t) \cos(\omega t)\, dt / \int_0^\infty F(t)\, dt \quad (7)$$

The lifetime distribution models were fitted to the experimental phase and modulation data by finding the parameters that minimized the reduced χ^2 where

$$\chi^2 = [1/(2n - f - 1)]\sum(m_i - c_i)^2/s_i^2 \quad (8)$$

Here m_i values are the measured phase ($i = 1$) or modulation ($i = 2$) values, and c_i values are the corresponding calculated values for the phase angle and modulation, n is the number of modulation frequencies, f is the number of parameters, and s_i values are the corresponding standard deviations of the measurements.

Lifetime-Resolved Emission Anisotropies. The emission anisotropy of the tryptophan residue in micelles was measured as a function of added collisional quencher. Fluorescence anisotropies were measured on the SLM 4800 spectrofluorometer with Glan–Thompson calcite prism polarizers in the L-format, excitation at 300 nm (8-nm slits), and emission observed through an Ealing 35-3011 interference filter (center 350.6, bandwidth 10.2 nm). Alignment of the polarizers was confirmed by measuring the polarization of a dilute glycogen solution. The steady-state anisotropy of the fluorescence signal was calculated from measurements of the parallel (I_{VV}) and perpendicular (I_{VH}) emission signals with the excitation polarizer oriented vertically. The G factor for the detection system is defined as I_{HV}/I_{HH} where the intensities are measured with a horizontal polarizer in the excitation path and an emission polarizer oriented horizontally (I_{HH}) or vertically (I_{HV}). The anisotropy, $r = (I_{VV} - GI_{VH})/(I_{VV} + 2GI_{VH})$.

The anisotropy of the tryptophan residue in a protein decays by overall rotational motion of the protein (or lipid–protein complex), with correlation time ϕ_P, and by segmental motions of the tryptophan within the protein matrix, with correlation time ϕ_T. The anisotropy is given by

$$r = \alpha r_0/(1 + \tau/\phi_T + \tau/\phi_P) + r_0(1 - \alpha)/(1 + \tau/\phi_P) \quad (9)$$

where α is the fraction of the anisotropy that decays due to segmental motions of the protein, τ is the lifetime, and r_0 [0.31 at 300 nm; Eftink (1983)] is the limiting anisotropy in the absence of motion, where ϕ is infinite or $\tau = 0$.

For a lipid–peptide micelle where $\phi_P \gg \tau$, eq 9 simplifies to (Maliwal et al., 1986)

$$r = (1 - \alpha)r_0 + \phi_T(r_0 - r)/\tau \quad (10)$$

Thus, a plot of r vs $(r_0 - r)/\tau$ gives a slope of ϕ_T and an intercept $r(0) = (1 - \alpha)r_0$.

Analytical Methods. Protein was determined from the extinction coefficient of the peptide at 280 nm. Phospholipid concentrations were measured by analysis of inorganic phosphorus following digestion in perchloric acid (Bartlett, 1959).

Results

Characterization of Micelles. Micelles were prepared by incubating 18As and DMPC at various weight ratios of peptide to lipid. Attempts to separate the micelles from unbound peptide by gel filtration chromatography were unsuccessful: although the micelles eluted as a single peak, the peptide:lipid ratio in micelles isolated by gel filtration decreased when the micelles were passed over the column a second time. This is presumably the result of the loss of free peptide which is in

Table I: Acrylamide Quenching of 18As/DMPC Micelles[a]

peptide:lipid weight ratio	τ (ns)	k_q(intensity) × 10^{-9} (M^{-1} s^{-1})	k_q(lifetime) × 10^{-9} (M^{-1} s^{-1})	γ	E_a (kcal/mol)
1:1	3.12	0.87 ± 0.03	0.46 ± 0.01	0.110	6.7
1:2	3.24	0.69 ± 0.07	0.42 ± 0.02	0.087	6.8
1:3	3.31	0.51 ± 0.01	0.38 ± 0.01	0.065	7.0
1:5	3.61	0.42 ± 0.05	0.28 ± 0.01	0.053	12.7
1:10	3.99	0.38 ± 0.03	0.30 ± 0.02	0.048	13.3

[a] Acrylamide quenching was measured at 26 °C, and the rate constants were calculated as described under Experimental Procedures. Lifetimes were measured by the phase method at 18 MHz. The quenching efficiency, γ, is k_q(intensity)/k_d, where k_d is the diffusion-limited rate constant (7.9 × 10^9 M^{-1} s^{-1}).

equilibrium with bound peptide even after isolation of the micelles. For this reason, unfractionated mixtures of peptide and lipid were used, and the amount of free peptide in equilibrium with the micelles was measured by separation of bound and free peptide by centrifugal filtration (Centricon 30). For equal weights of peptide and lipid (1:1 micelles), <8% of the peptide was not bound to lipid when the total peptide concentration was 0.1 mg/mL (the concentration used for fluorescence measurements). At peptide:lipid ratios ≤1:2, peptide was nearly quantitatively bound (<2% free). This small amount of free peptide does not have dramatic effects on measurements of peptide conformation: since the concentration of free peptide is expected to vary with the overall concentration of micelles, a significant concentration dependence might be expected in the circular dichroic (CD) spectra. However, the CD spectra of the peptide are independent of concentration in the range 0.05–0.25 mg of peptide/mL for 1:1 micelles.

At all peptide:lipid ratios examined, the mixtures were visibly clear at the concentrations employed for fluorescence measurements. By electron microscopy, disk-shaped micelles of 4.2-nm thickness were observed, corresponding to single bilayers (Hauser et al., 1974), stacked to form long chains. The average diameter of the micelles increased with decreasing peptide:lipid ratios from 12.0 ± 0.4 nm at 1:1 up to a maximum diameter of 48.7 ± 1.0 nm at 1:13 weight ratios. For a 1:5 ratio, the diameter was 22.7 ± 0.6 nm. A unimodal distribution of sizes was obtained by gel filtration at all peptide:lipid ratios. Thus, a small number of discrete size classes are not observed, consistent with the large number of peptides expected within each micelle (~25 peptide molecules per micelle for 1:1 and ~70 peptide molecules per micelle for 1:10, based on the measured diameters of the micelles). Micellar forms are observed at all peptide:lipid ratios examined by electron microscopy. Similar results have been reported by Anantharamaiah et al. (1985) who employed gel filtration, nondenaturing gradient gel electrophoresis, and electron microscopy.

Fluorescence Quenching. The fluorescence of 18As alone or in DMPC micelles is dominated by the fluorescence of its single tryptophan residue; the shapes of the emission spectra do not differ with excitation at 280 and 295 nm. To minimize potential contributions of tyrosine, an excitation wavelength of 295 nm was used in steady-state measurements, and 289 nm was used in multiple-frequency lifetime measurements. After a 30-min incubation of DMPC liposomes with the peptide at a weight ratio of 1:1 (peptide:lipid), the fluorescence emission maximum is shifted from 353 nm (peptide alone) to 346 nm (peptide + DMPC). This time period corresponds to the end point for clearing of the liposomes as measured by a decrease in turbidity of the mixture. After a 24-h incubation of the peptide mixture with DMPC at 26 °C, the fluorescence emission of the mixture is further blue-shifted to 337 nm. A small further shift to 334 nm is observed when the lipid concentration is increased to a 1:5 peptide:lipid weight ratio. In addition, at lower peptide:lipid ratios, the fluorescence lifetime (measured at 18 MHz) increases (Table I) as does the intensity of the fluorescence signal.

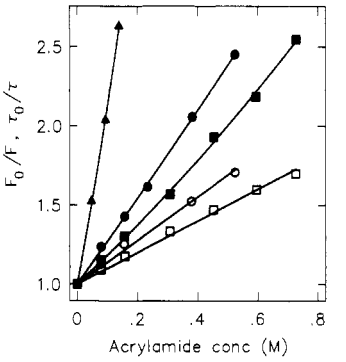

FIGURE 1: Fluorescence quenching by acrylamide. Intensity quenching measurements: (▲) 18As; (●) 18As/DMPC, 1:1; (■) 18As/DMPC, 1:5. Lifetime measurements: (○) 18As/DMPC, 1:1; (□) 18As/DMPC, 1:5.

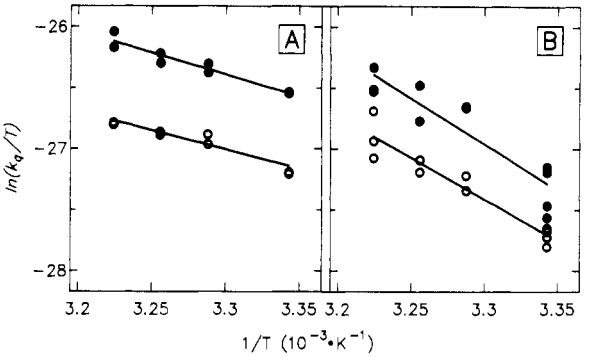

FIGURE 2: Temperature dependence of acrylamide quenching: (●) intensity measurements; (○) lifetime measurements. Panel A, 18As/DMPC, 1:1; panel B, 18As/DMPC, 1:5.

Figure 1 shows the quenching by acrylamide of peptide in solution and in peptide/lipid micelles at weight ratios of 1:1 and 1:5. The rate constant for acrylamide quenching of 18As in the absence of lipid at 26 °C is 6.20 × 10^9 M^{-1} s^{-1} and γ = 0.78. The intensity quenching data (F_0/F) are nearly linear with increasing quencher concentration; the static quenching constants (V) are <0.3 M^{-1} for all peptide:lipid ratios, indicating that static quenching does not contribute significantly to the quenching kinetics (Eftink & Ghiron, 1976). Furthermore, quenching of 1:1 micelles in the presence of 50% glycerol did not have a significant effect on the quenching rate (relative rates: +glycerol/−glycerol = 1.06) as expected for collisional quenching. That no rapidly quenched component is observed supports the contention that free peptide in the samples is minimal; the lifetime quenching data are linear as expected from eq 1. The rate constants (k_q) and relative efficiencies (γ) for quenching by acrylamide are given in Table I. With decreasing peptide:lipid ratio, the rate constants for

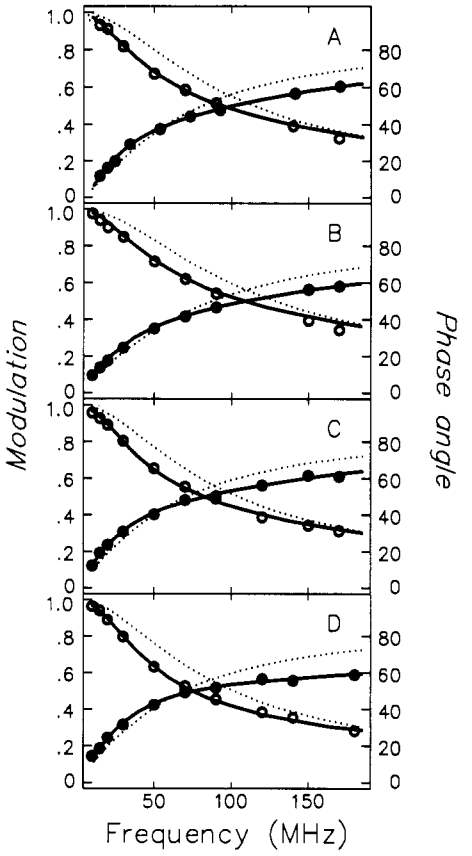

FIGURE 3: Lifetime modulation ratios (O) and phase angles (●) from measurements at frequencies from 10 to 180 MHz. The data were fit by a single-exponential model (dotted line) or a double-exponential model (solid line) as described under Experimental Procedures. (A) 18As/DMPC, 1:1; (B) 18As/DMPC, 1:2; (C) 18As/DMPC, 1:5; (D) 18As/DMPC, 1:10. Excitation was at 290 nm.

quenching and the relative efficiencies of quenching decrease.

The effect of temperature on the rate of quenching for 1:1 and 1:5 micelles is presented in Figure 2. A summary of the activation energies measured for acrylamide quenching (Table I) indicates that E_a increases with decreasing peptide:lipid ratio. There is no evidence for a break in the Eyring plots of the quenching data [see Gomez-Fernandez et al. (1985) for the temperature dependence of acrylamide quenching of Ca^{2+}-ATPase in DMPC] even though at weight ratios of 1:2 and above a broad lipid-phase transition centered at 26 °C is observed (L. R. McLean, unpublished data; Anantharamaiah et al., 1985).

Fluorescence Lifetimes. The phase and modulation lifetimes of peptide/DMPC complexes at weight ratios from 1:1 to 1:10 (peptide/lipid) at 18 MHz do not differ with excitation at 290 or 295 nm. Multifrequency data (10–180 MHz) were fitted to a discrete exponential model (eq 2) and a Lorentzian probability distribution model (eq 3). The fit of the data to the models was judged from examination of χ^2 and the difference between the experimental and theoretical phase and modulation values (residuals) as a function of modulation frequency. Peptide alone was best fit by either a two-exponent model (τ_1 = 2.76 ns, τ_2 = 0.88 ns, f_1 = 0.56) or a single Lorentzian (center, c = 1.58 ns; width, ω = 1.10 ns). For the discrete exponential model, a single exponential fit the data poorly (Figure 3, dotted line). For all peptide:lipid ratios, addition of a second exponential component to the decay process improved the overall fit of the decay process to the phase and modulation data (Figure 3, solid line) and decreased χ^2 (Table II). Addition of a third component did not decrease χ^2 significantly. To test for a light-scattering contribution to

Table II: χ^2 for Lifetime Models[a]

sample	single exponential	double exponential	Lorentzian distribution	global analysis
1:1	62.0	2.90	1.76	6.00
1:2	70.2	1.26	3.46	4.67
1:5	51.6	2.05	2.67	1.87
1:10	79.8	1.85	12.73	8.77

[a] Lifetime distributions were calculated from phase and modulation data measured at 10 frequencies from 10 to 180 MHz and at 26 °C with an excitation wavelength of 290 nm. The standard deviations of the phase and modulation values were 0.6 and 0.01, respectively.

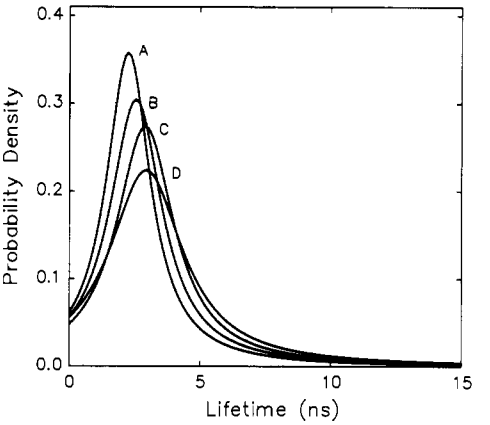

FIGURE 4: Lifetime distributions determined by analysis of the data in Figure 3 with a Lorentzian distribution model. Line A is 1:1 18As/DMPC, B is 1:2, C is 1:5, and D is 1:10.

the lifetimes, the data were compared for a two-component exponential decay process with and without an additional fixed 0.001-ns component. With the additional component in 1:10 micelles, τ_1 = 4.22 ± 0.11 ns, τ_2 = 0.63 ± 0.15 ns, and f_1 = 0.83 ± 0.02; without the light-scattering component, τ_1 = 4.22 ± 0.11 ns, τ_2 = 0.64 ± 0.07 ns, and f_1 = 0.83 ± 0.01. Thus, including the light-scattering component did not improve the fit even at the highest lipid concentration examined. At all other peptide:lipid ratios, the contribution of the 0.001-ns component was <1%. Thus, light scattering did not appear to contribute significantly to the lifetime distributions, and the data did not justify addition of a third component.

Data were also analyzed with a Lorentzian lifetime distribution model. The χ^2 values for the Lorentzian distribution and the double-exponential model are nearly the same for peptide:lipid ratios up to 1:5 (Table II). However, the double-exponential model provides considerably improved fit for 1:10 micelles. Including a second Lorentzian component in the distribution for 1:10 micelles reduces χ^2 to 1.78 and increases the lifetime of the longer component further. For a two-component Lorentzian distribution model and 1:10 micelles, the longer lifetime component is centered at 4.28 ns and contributes 82.1% to the decay; the shorter component is centered at 0.69 ns. The shapes of the Lorentzian distributions are shown in Figure 4.

The effect of peptide mole fraction within the micelles on the lifetime data is shown in Figure 5. Data calculated with a double-exponential model are in Figure 5A; the same data calculated by the Lorentzian distribution model are in Figure 5B. For a double-exponential model, the lifetimes of both components are relatively independent of peptide mole fraction. At the lowest peptide mole fraction (1:10 peptide:lipid weight ratio), both the shorter and longer lifetime components decrease somewhat in the double-exponential model, and the contribution of the longer lifetime component is increased considerably. The widths of the Lorentzian distribution of lifetimes decrease with increasing peptide mole fraction; the

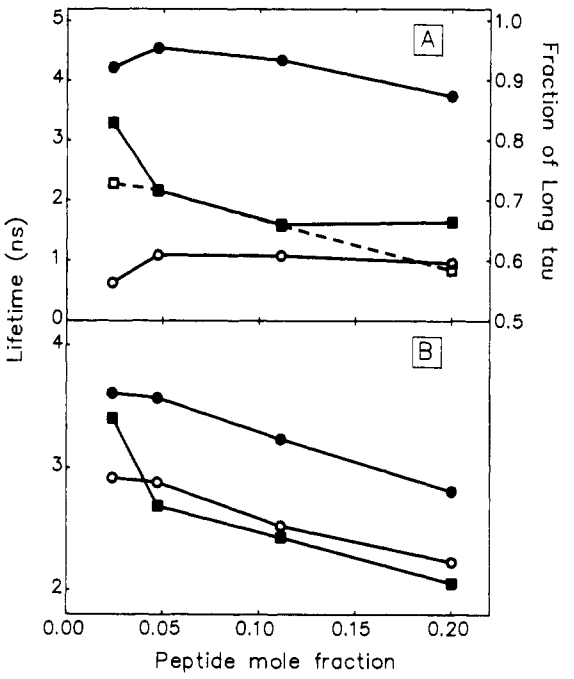

FIGURE 5: Summary of lifetimes as a function of mole fraction of peptide in the micelles. In panel A are the lifetimes of component 1 (●) and component 2 (○) and the fraction of component 1 (■) calculated for a double-exponential model and the fraction of the long-lifetime component (□) calculated by global analysis. In panel B are the widths (■) and central values (○) of the Lorentzian distribution fitted to the same data. The average lifetimes calculated from the double-exponential decay model are also shown (●).

width of the distribution increases more rapidly at low peptide mole fractions. The center lifetime of the Lorentzian distribution decreases with increasing peptide mole fraction. The average fluorescence lifetimes, calculated from the double-exponential model (Figure 5B), are somewhat greater than the center values for the Lorentzian distribution, but follow the same pattern.

The fluorescence decay data at various peptide mole fractions were also analyzed in a simultaneous (global) manner using the program of Beechem and Gratton (1988). Here a double-exponential decay was assumed, and the two decay times were linked to be the same for each data set; the fractional intensities were allowed to vary in the analysis. The globally fitted lifetimes were $\tau_1 = 4.5$ ns and $\tau_2 = 1.1$ ns. As shown by the dashed line in Figure 5, the fractional intensity of the long-lived component was found to decrease monotonically with increasing peptide mole fraction. Thus, the global analysis supports the individual fitting parameters presented in Figure 5.

The potential contribution of free peptide to the analysis of the lifetime data was calculated by including a free peptide component in the data analysis. For 1:1 micelles, ~8% of the peptide is not associated with lipid. The contribution of this peptide to the phase and modulation data analysis was calculated by a four-component exponential analysis, fixing the lifetimes of two components to correspond to free peptide, $\tau_3 = 2.76$ ns and $\tau_4 = 0.88$ ns, and the fractions to 8%; thus, $f_3 = 0.08 \times 0.56$ and $f_4 = 0.08 \times 0.44$ where 0.08 is the fraction of free peptide and the values correspond to those measured for 18As in the absence of lipid. Without the free peptide component included, the micelles gave $\tau_1 = 3.75$ ns, $\tau_2 = 0.97$ ns, and $f_1 = 0.66$; with the free peptide component, $\tau_1 = 3.81$ ns, $\tau_2 = 0.98$ ns, and $f_1 = 0.66$. Similarly, a two-component Lorentzian analysis was employed, fixing $c_2 = 1.58$ ns, $\omega_2 = 1.10$ ns, and $f_2 = 0.08$. In this analysis, without the peptide component, the micelles gave $c_1 = 2.24$ ns and $\omega_1 = 2.06$ ns; with the peptide component, $c_1 = 2.33$ ns and $\omega_1 = 2.11$ ns. Thus, the free peptide in equilibrium with the micelles contributed little to the observed lifetimes, and the changes in fluorescence of the tryptophan residues as a function of peptide:lipid ratio are not simply the result of a change in equilibrium between free and bound peptide. In fact, even smaller differences were obtained at higher peptide:lipid ratios.

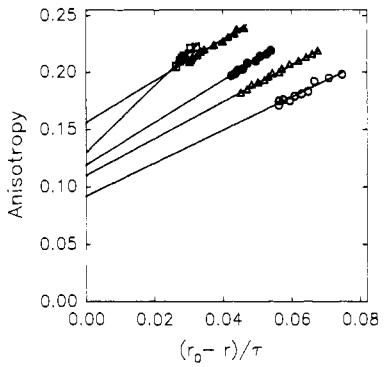

FIGURE 6: Lifetime-resolved anisotropies of 18As/DMPC micelles: (○) 1:1 at 26 °C; (●) 1:1 at 37 °C; (△) 1:5 at 26 °C; (▲) 1:5 at 37 °C; (□) 1:8 at 26 °C. Measurements of the steady-state anisotropy of the peptide with excitation at 300 nm were made as a function of added acrylamide.

Table III: Lifetime-Resolved Anisotropies of 18As/DMPC Micelles[a]

sample	r	$r(0)$	ϕ_T (ns)	α
1:1 at 26 °C	0.181	0.119 ± 0.004	1.86 ± 0.09	0.62 ± 0.01
1:1 at 37 °C	0.164	0.092 ± 0.008	1.44 ± 0.12	0.71 ± 0.02
1:5 at 26 °C	0.202	0.156 ± 0.002	1.83 ± 0.07	0.50 ± 0.01
1:5 at 37 °C	0.182	0.110 ± 0.002	1.61 ● 0.03	0.64 ± 0.01
1:8 at 26 °C	0.205	0.130 ± 0.009	2.92 ± 0.33	0.58 ± 0.02

[a] r is the steady-state anisotropy in the absence of quencher, $r(0)$ is the intercept of a plot of r vs $(r_0 - r)/\tau$, and α is the fraction of rapidly decaying anisotropy with correlation time, ϕ_T. The error of individual r values is ±0.003. The error of α values is the error of $r(0)/r_0$.

Lifetime-Resolved Emission Anisotropies. The effect of peptide:lipid ratio on nanosecond rotational motions of the tryptophan residue in 18As was examined by measuring the fluorescence emission anisotropy of the peptide as a function of added collisional quencher. Excellent fits of the data to eq 10 were obtained (Figure 6). When the data were fit to eq 9 (which includes contributions from the overall rotational motion of the micelle), varying ϕ_P from 10 to 100 ns had only a minimal effect on the fitted values. Thus, the data do not provide information on the value of ϕ_P, other than that the assumptions underlying the use of eq 9 are valid. A summary of the fitted parameters is given in Table III. Similar nanosecond motions for tryptophan residues in apolipoproteins in phosphatidylcholines and detergents have been observed (Maliwal et al., 1985; Jonas et al., 1982). No significant change in the rotational correlation time for rapid nanosecond motions (ϕ_T) is observed on decreasing the peptide:lipid ratio from 1:1 to 1:5 at 26 °C; at 37 °C, ϕ_T is increased minimally. A further decrease in peptide:lipid ratio, to 1:8, increases ϕ_T dramatically, suggesting more hindered motions of the residue. The fraction of anisotropy decay due to rapid motions is decreased significantly on going from 1:1 to 1:5 ratios at both 26 and 37 °C.

Discussion

The present experiments focus on the effect of peptide:lipid ratio on the tryptophan environment of a model amphipathic helical peptide (18As) in DMPC. An increase in the diameter of the micelles with decreasing peptide:lipid ratio was observed

by electron microscopy, confirming the data of Anantharamaiah et al. (1985). In addition, with decreasing peptide:lipid ratio: (1) the average fluorescence lifetime of the single tryptophan residue in the peptide is increased as a result of a decrease in the fractional contribution of a 1.1-ns (short) lifetime component and an increase in the contribution of a 4.5-ns (long) lifetime component in the fluorescence decay, on the basis of a global analysis of multifrequency phase fluorometry data; (2) the rate of acrylamide quenching of tryptophan in the peptide is reduced; (3) the emission maximum of the tryptophan is shifted to shorter wavelengths and (4) the rate and fraction of the anisotropy decay which are due to rapid (nanosecond) rotational motions of the tryptophan are decreased. These changes are not the result of an increase in free peptide at higher peptide:lipid ratios since the small amount of unbound peptide in equilibrium with peptide bound to the lipid cannot account for the observed dependence of the lifetimes on peptide:lipid ratio. In addition, the fluorescence quenching data show that free peptide does not contribute significantly to the quenching kinetics.

It is tempting to directly relate the quenching process to the fluorescence lifetime distribution. Thus, the increase in the fraction of the longer lifetime component in the peptide in the presence of decreasing peptide mole fraction may be the result of a more solvent-shielded environment for the tryptophan residue. This conclusion is consistent with the decreased acrylamide fluorescence quenching rates observed for 18As in the lipid micelles relative to peptide in solution and with the decrease in quenching rate with decreasing peptide:lipid ratio. As the micelle diameter increases (decreasing peptide:lipid ratio), the proportion of tryptophan residues in the more shielded environment increases, resulting in an increase in the width of the lifetime distribution or an increase in the contribution of the longer lifetime component.

The shorter lifetime component may be due to interactions between the indole rings of neighboring tryptophan rings which are expected to more closely approach each other as the curvature of the micelle is decreased (at low peptide:lipid ratios). Alternatively, quenching of the tryptophan by neighboring charged residues may give rise to the short lifetime component. Such interactions might explain the decrease in the lifetime of the short-lifetime component at low peptide:lipid ratios in the micelle. A similar short-lifetime component has been observed in gramicidin A in lysolecithin micelles (Masotti et al., 1986) and in apoC-I/DMPC micelles (Jonas et al., 1982).

The lack of effect of glycerol on the rate of acrylamide quenching and the high activation energy for quenching observed in the micelles (6.7–13.3 kcal/mol) support a mechanism in which diffusion of acrylamide through a nonpolar matrix is the rate-determining step for acrylamide quenching (Eftink & Hagaman, 1985, 1987); by contrast, the activation energy for quenching of indole derivatives in water is on the order of 3.7 kcal/mol (Eftink & Ghiron, 1976). Acrylamide may penetrate the micelles through holes formed in the lipid matrix, between adjacent peptide helices, or at the phase boundary between peptide and lipid. For penetration through the lipid phase, it is expected that quenching rates would decrease as the packing of the molecules in the micelle becomes tighter (at lower peptide:lipid ratio). However, the low solubility of acrylamide in lipid and its inability to quench nonpolar fluorescence probes in liposomes (L. R. McLean, unpublished data) suggest that diffusion within the lipid matrix is not the rate-limiting step for quenching. Rather, the data support a model in which the decrease in the rate of quenching with decreasing peptide:lipid ratio is the result of an increased activation energy barrier for hole formation on the nanosecond time scale at the peptide–lipid interface or between peptide helices. Such fluctuations near the tryptophan residue of 18As would allow penetration of arylamide during the lifetime of the excited state. Acrylamide quenching of Ca^{2+}-ATPase in PC vesicles may also proceed by diffusion between adjacent peptide helices, but within the protein interior (Gomez-Fernandez et al., 1985).

Since the micelle diameter increases with decreased peptide:lipid ratio, the data suggest that the tryptophan residue of 18As in DMPC becomes less accessible to the aqueous phase solvent as the diameter of the micelle increases. By contrast to these data on a short amphipathic α-helical peptide, addition of DMPC to apolipoprotein A-I (apoA-I) has little effect on the rate of acrylamide quenching (Mantulin et al., 1986), and the conformation of apoA-I in DMPC micelles is relatively independent of micellar lipid:protein ratio (Wetterau & Jonas, 1983; Jonas et al., 1980; Jonas & McHugh, 1984). However, in both apoA-I/DMPC and 18As/DMPC micelles, the choline *N*-methyl proton resonance of the lipid is shifted progressively downfield with increasing micelle diameter (Brouillette et al., 1984; Anantharamaiah et al., 1985). These data have been interpreted in terms of two lipid environments whose distribution changes with incresing micelle diameter. Although such a model may be reasonable for interpreting the lipid data, it is inadequate for explaining the variation in tryptophan environment observed with increasing micelle diameter. Presumably, those structural changes in the micelle which lead to the downfield shift of the choline *N*-methyl proton resonance with increasing micelle diameter also contribute to the increased solvent shielding and decreased rotational freedom of the tryptophan residue of the peptide.

An alternative model for the effect of micelle diameter on both peptide and lipid dynamics within the micelle postulates a gradual change in the dynamics of the lipid and the peptide in the micelle. Rather than a rapid two-state equilibrium between lipid adjacent to peptide and lipid in a more central region of the micelle (Brouillette et al., 1984), the hydration of the choline head groups may suffer a progressive change with micelle diameter leading to a progressive downfield shift in the *N*-methyl resonance. This model would take into account changes in the dynamics of the tryptophan residue and its local interactions with lipid. By analogy to structural fluctuations in lipid monolayers which give rise to local low surface pressures and hole formation (Blank & Britten, 1965; Phillips et al., 1975), the probability of hole formation in the micelle may then depend upon the lateral compressibility between amphipathic helices or between helices and adjacent phospholipid molecules. Since tighter packing is expected between helices in larger micelles (much like a tightly packed monolayer), the compressibility will be low, and the relaxation processes for the tryptophans are expected to slow with increasing micelle diameter, thereby increasing the fraction of the fluorescence decay which is due to the longer lifetime component. Thus, the data support a dynamic view of the peptide/lipid micelle in which structural fluctuations occur on the nanosecond time scale and where the lipid and, possibly the peptide, is not necessarily confined to discrete regions within the micelle.

ACKNOWLEDGMENTS

We thank Dr. John Coutant for analysis of the peptides by mass spectrometry, Dr. D. Jean Sprinkle for electron microscopy, Susan Treadway for preparation of the manuscript, and Andrew Stein for preparation of the figures.

REFERENCES

Alcala, J. R., Gratton, E., & Prendergast, F. G. (1987) *Biophys. J. 51*, 587–596.

Anantharamaiah, G. M., Jones, J. L., Brouillette, C. G., Schmidt, C. F., Chung, B. H., Hughes, T. A., Bhown, A. S., & Segrest, J. P. (1985) *J. Biol. Chem. 260*, 10248–10255.

Argiolas, A., & Pisano, J. J. (1985) *J. Biol. Chem. 260*, 1437–1444.

Bartlett, G. R. (1959) *J. Biol. Chem. 234*, 466–468.

Beechem, J. M., & Gratton, E. (1988) *Proc. SPIE–Int. Soc. Opt. Eng. 909*, 70–81.

Blank, M., & Britten, J. S. (1965) *J. Colloid Sci. 20*, 789–800.

Brouillette, C. G., Jones, J. L., Ng, T. C., Kercret, H., Chung, B. H., & Segrest, J. P. (1984) *Biochemistry 23*, 359–367.

Day, C. E., & Levy, R. I. (1969) *J. Theor. Biol. 23*, 387–399.

Eftink, M. (1983) *Biophys. J. 43*, 323–334.

Eftink, M. R., & Ghiron, C. A. (1976) *Biochemistry 15*, 672–680.

Eftink, M. R., & Hagaman, K. A. (1985) *Biophys. Chem. 22*, 173–180.

Eftink, M. R., & Hagaman, K. A. (1987) *Biophys. Chem. 25*, 277–282.

Georghiou, S., Thompson, M., & Mukhopadhyay, A. K. (1982) *Biochim. Biophys. Acta 688*, 441–452.

Gomez-Fernandez, J. C., Baena, M. D., Teruel, J. A., Villalain, J., & Vidal, C. J. (1985) *J. Biol. Chem. 260*, 7168–7170.

Hauser, H., Henry, R., Leslie, R. B., & Stubbs, J. M. (1974) *Eur. J. Biochem. 48*, 583–594.

Jameson, D. M., Gratton, E., & Hall, R. D. (1984) *Appl. Spectrosc. Rev. 20*, 55–106.

Jonas, A., & McHugh, H. T. (1984) *Biochim. Biophys. Acta 794*, 361–372.

Jonas, A., Drengler, S. M., & Patterson, B. W. (1980) *J. Biol. Chem. 255*, 2183–2189.

Jonas, A., Privat, J.-P., Wahl, P., & Osborne, J. C., Jr. (1982) Biochemistry *21*, 6205–6211.

Kaiser, E. T., & Kezdy, F. J. (1984) *Science 223*, 249–255.

Kanellis, P., Romans, A. Y., Johnson, B. J., Kercret, H., Chiovetti, R., Jr., Allen, T. M., & Segrest, J. P. (1980) *J. Biol. Chem. 255*, 11464–11472.

Lakowicz, J. R., Laczko, G., Cherek, H., Gratton, E., & Limkeman, M. (1984) *Biophys. J. 46*, 463–477.

Maliwal, B. P., Cardin, A. D., Jackson, R. L., & Lakowicz, J. R. (1985) *Arch. Biochem. Biophys. 236*, 370–378.

Mantulin, W. W., Pownall, H. J., & Jameson, D. M. (1986) *Biochemistry 25*, 8034–8042.

Masotti, L., Cavatorta, P., Sartor, G., Casali, E., & Szabo, A. G. (1986) *Biochim. Biophys. Acta 862*, 265–272.

Massey, J. B., Gotto, A. M., Jr., & Pownall, H. J. (1981) *Biochemistry 20*, 1575–1584.

McLean, L. R., & Hagaman, K. A. (1988) *Biochim. Biophys. Acta 959*, 201–205.

Morrisett, J. D., Jackson, R. L., & Gotto, A. M., Jr. (1977) *Biochim. Biophys. Acta 472*, 93–133.

Parker, C. A. (1968) *Photoluminescence of Solutions*, pp 220–222, Elsevier, New York.

Perutz, M. F., Kendrew, J. C., & Watson, H. C. (1965) *J. Mol. Biol. 13*, 669–678.

Phillips, M. C., Graham, D. E., & Hauser, H. (1975) *Nature 254*, 154–155.

Segrest, J. P., Jackson, R. L., Morrisett, J. D., & Gotto, A. M., Jr. (1974) *FEBS Lett. 38*, 247–253.

Spencer, R. D., & Weber, G. (1969) *Ann. N.Y. Acad. Sci. 158*, 361–376.

Swaney, J. B. (1980) *J. Biol. Chem. 255*, 877–881.

Tall, A. R., Small, D. M., Deckelbaum, R. J., & Shipley, G. G. (1977) *J. Biol. Chem. 252*, 4701–4711.

Wetterau, J. R., & Jonas, A. (1983) *J. Biol. Chem. 258*, 2637–2643.